

# Determination of the strong coupling constant and the Collins–Soper kernel from the energy–energy correlator in $e^+e^-$ collisions

Zhong-Bo Kang,<sup>1, 2, 3,\*</sup> Jani Penttala,<sup>1, 2, †</sup> and Congyue Zhang<sup>1, 2, ‡</sup>

<sup>1</sup>*Department of Physics and Astronomy, University of California, Los Angeles, CA 90095, USA*

<sup>2</sup>*Mani L. Bhaumik Institute for Theoretical Physics,*

*University of California, Los Angeles, CA 90095, USA*

<sup>3</sup>*Center for Frontiers in Nuclear Science, Stony Brook University, Stony Brook, NY 11794, USA*

We have conducted the first simultaneous global fit of the strong coupling constant  $\alpha_s$  and the Collins–Soper (CS) kernel using the energy–energy correlators (EEC) of  $e^+e^-$  collisions in the back-to-back limit. This analysis, based on the transverse-momentum-dependent (TMD) factorization of EEC at next-to-next-to-next-to-leading logarithmic ( $N^3LL$ ) accuracy, yields  $\alpha_s$  consistent with the world average. We have tested two different parametrizations for the non-perturbative CS kernel and found both to align with results obtained from lattice QCD and fits on semi-inclusive deep inelastic scattering and Drell–Yan process.

**Introduction.** One of the most important parameters in quantum chromodynamics (QCD) is the strong coupling constant  $\alpha_s$ , which describes the strength of strong interactions. Its precise value depends on the relevant momentum scale of the underlying process, and this momentum-scale dependence can be calculated perturbatively using a renormalization group equation [1–7]. This equation requires, however, an initial condition that has to be fitted to the experimental data, and usually this initial condition is chosen as the value of the coupling constant at the  $Z$ -boson mass,  $\alpha_s(m_Z)$ . This value of the strong coupling constant can then be used to describe any QCD interaction, provided that the momentum scale is large enough for the process to be perturbative.

The strong coupling constant has been previously extracted from a plethora of different processes [8], demonstrating the perturbative consistency of QCD. In terms of determining the precise value of the coupling constant, an especially powerful class of processes has turned out to be event-shape observables [9–11] where, instead of studying the individual produced particles, one examines the overall geometry of the final-state distribution. This means that event-shape observables are generally less sensitive to the non-perturbative (NP) hadronization of the final-state particles, allowing one to focus more on other parts of the collision process.

The process of interest in this Letter is the energy–energy correlator (EEC) event-shape observable which describes angular correlations between pairs of produced particles. EEC was one of the first infrared-safe observables for QCD [12, 13], and it has already been studied extensively at different experiments [14–29]. Recently, it has garnered renewed interest in precision QCD research, probing both perturbative and non-perturbative dynamics in collisions ranging from  $e^+e^-$  annihilation and deep inelastic  $ep$  scattering to proton–proton and heavy-ion collisions [30]. Two kinematic limits of EEC have been extensively studied and have shown important physics insights of its own [31, 32]: the collinear limit [33], where

a pair of particles moves in the same or nearly collinear direction, and the back-to-back limit, which focuses on particle pairs with momenta pointing in opposite directions.

In this Letter, we focus on the back-to-back limit of EEC. This limit can be described efficiently using the framework of transverse-momentum-dependent (TMD) factorization [34, 35], which factorizes the collision into separate calculable parts of different momentum scales. To account for non-perturbative hadronization effects, we introduce the NP Sudakov factor and the NP Collins–Soper (CS) kernel, also known as the rapidity anomalous dimension, which is universal across different processes [34–36]. A precise determination of the CS kernel is of especially high interest due to its crucial role in understanding the rapidity evolution of TMD parton distributions functions (PDF) and fragmentation functions (FF), and it has emerged as a central focus in recent lattice QCD calculations [36–43]. Understanding the NP CS kernel is thus crucial for any study based on TMD factorization, especially for imaging nuclear structure in the transverse momentum plane—one of the major science goals of the future Electron–Ion Collider [44–46].

In this Letter, we present a simultaneous fit of both the strong coupling constant and the Collins–Soper kernel at next-to-next-to-next-to-leading logarithmic ( $N^3LL$ ) accuracy to the EEC data from  $e^+e^-$  collisions. This marks the first extraction of the CS kernel from an observable that is independent of non-perturbative parton distribution and fragmentation functions, thereby minimizing reliance on other non-perturbative components in the calculation. This highlights the EEC as a particularly clean observable for precision studies of QCD. Our fit for the non-perturbative part of the CS kernel can be applied to other processes described using TMD factorization, allowing for more accurate analyses of TMD parton distributions and fragmentation functions.

**Theoretical Formalism.** The EEC observable is defined as an event shape to measure the energy-weighted

angular distance between pairs of particles [32]:

$$\frac{d\Sigma}{d\chi} = \sum_{ij} \int d\sigma \frac{E_i E_j}{Q^2} \delta(\chi - \theta_{ij}). \quad (1)$$

Here  $E_i$  is the energy of the particle  $i$  and  $Q$  is the center-of-mass energy of the collision. The sum goes over all final-state particles, and  $\theta_{ij}$  is the angle between the the final-state particles  $i$  and  $j$ . EEC is also commonly defined in the variable  $z = (1 - \cos \chi)/2$ . Higher-order calculations of the EEC involve singular contributions of the form  $\log^n(1 - z)$  that must be resummed in the back-to-back limit where  $z \rightarrow 1$ , whereas the non-singular contributions remain unchanged. We can write the EEC as

$$\frac{d\Sigma}{d\chi} = \frac{\sin(\chi)}{2} \frac{d\Sigma}{dz}, \quad \frac{d\Sigma}{dz} = \frac{d\Sigma^{\text{res}}}{dz} + \frac{d\Sigma^{\text{nons}}}{dz}, \quad (2)$$

where  $\sigma^{\text{res}}$  and  $\sigma^{\text{nons}}$  correspond to the resummed singular and non-singular contributions to the EEC. The non-singular contribution has been computed analytically at NLO in [47], and the fixed-order EEC has been obtained numerically at NNLO [48]. In this Letter, we use the NLO result. The resummation of the large logarithms in the back-to-back limit can be done using the TMD factorization and leads to the expression [32]

$$\begin{aligned} \frac{d\Sigma^{\text{res}}}{dz} &= \frac{\hat{\sigma}_0}{8} H_{q\bar{q}}(Q, \mu_H^i) \int_0^\infty d(bQ)^2 J_0(bQ\sqrt{1-z}) \quad (3) \\ &\times J_q^{\text{pert}}(b_*, \mu_J^i, \zeta^i) J_{\bar{q}}^{\text{pert}}(b_*, \mu_J^i, \zeta^i) \left( \frac{\zeta^f}{\zeta^i} \right)^{K(b, \mu^f)} e^{-2S_{\text{NP}}(b)} \\ &\times \exp \left\{ \int_{\mu_H^i}^{\mu^f} \frac{d\mu'}{\mu'} \gamma_H(Q, \mu') + 2 \int_{\mu_J^i}^{\mu^f} \frac{d\mu'}{\mu'} \gamma_J(\mu', \zeta^i) \right\}. \end{aligned}$$

Here  $\hat{\sigma}_0$  is the Born cross section of  $e^+ + e^- \rightarrow q + \bar{q}$ ,  $H_{q\bar{q}}$  is the hard function, and  $J_q$  ( $J_{\bar{q}}$ ) is the quark (anti-quark) jet function. The hard function and the jet functions satisfy the renormalization group equations for the momentum scale  $\mu$ , which is given by the hard anomalous dimension  $\gamma_H$  and jet anomalous dimension  $\gamma_J$ , respectively. The jet functions also depend on the rapidity scale  $\zeta$  through the CS evolution that is governed by the CS kernel  $K$ . Our resummation is performed at the  $N^3LL$  accuracy and relies on the 2-loop hard [49], jet [32], and soft [50] functions, the 3-loop non-cusp anomalous dimensions [50–52] and rapidity anomalous dimension [50, 53, 54], and the 4-loop beta function [55–58] and cusp anomalous dimension  $\Gamma_{\text{cusp}}$  [59–68]. We have implemented the standard  $b_*$  prescription [69, 70] to avoid the Landau pole of QCD, where  $b_* = b/\sqrt{1 + b^2/b_{\max}^2}$ , and we choose  $b_{\max} = 2e^{-\gamma_E}$  GeV $^{-1}$ . The CS kernel is defined as

$$\begin{aligned} K(b, \mu) &= -2 \int_{\mu_{b_*}}^\mu \frac{d\mu'}{\mu'} \Gamma_{\text{cusp}}[\alpha_s(\mu')] \\ &- 2D_{\text{pert}}(b_*, \mu_{b_*}) - 2D_{\text{NP}}(b), \quad (4) \end{aligned}$$

Collaboration	$Q$ (GeV)	$N_{\text{data}}$	$\chi^2$ (Fit 1)	$\chi^2$ (Fit 2)
OPAL [16]	91.2	30	12.4	12.4
SLD [14]	91.2	9	2.5	2.4
TOPAZ [17]	59.5	9	11.3	11.3
TOPAZ [17]	53.3	9	12.7	12.7
TASSO [18]	43.5	9	8.6	8.7
TASSO [18]	34.8	9	10.3	10.4
MARKII [21]	29.0	9	12.8	12.8
MAC [20]	29.0	9	14.2	14.3
Total		93	84.8	84.9

TABLE I. The experimental data used in the fits and the corresponding  $\chi^2$  values for the best fits.

where we also include the non-perturbative contribution  $D_{\text{NP}}$  that has to be modeled. The perturbative boundary term  $D_{\text{pert}}$  of the CS kernel can be found in [50]. The canonical initial scales which eliminate logarithmic terms in the hard and jet functions are given by

$$\mu_H^i = Q, \quad \mu_J^i = \mu_{b_*}, \quad \zeta^i = \mu_{b_*}^2, \quad (5)$$

where  $\mu_{b_*} = 2e^{-\gamma_E}/b_*$ . For the final scales, we set  $\mu^f = Q$  and  $\zeta^f = Q^2$ .

There are two main sources of NP contributions. Firstly, the jet function  $J_q$  is related to the TMD fragmentation function as follows:  $J_q(b, \mu, \zeta) = \sum_h \int_0^1 dz z D_{h/q}(z, b, \mu, \zeta)$ . Thus, when  $1/b \lesssim \Lambda_{\text{QCD}}$ , the jet function receives a NP contribution, and we incorporate it within the NP Sudakov factor:  $J_q = J_q^{\text{pert}} \times e^{-S_{\text{NP}}(b)}$ , where  $J_q^{\text{pert}}$  is the perturbative result [32] and for  $S_{\text{NP}}(b)$  we use the following form from [71]:

$$S_{\text{NP}}(b) = a_1 b^{a_2}. \quad (6)$$

The second NP source arises from the NP contribution  $D_{\text{NP}}(b)$  of the CS kernel  $K$  in Eq (4), and we inspect two different parametrizations:

$$D_{\text{NP}}^{\text{Fit } 1} = g_2 b b_*, \quad D_{\text{NP}}^{\text{Fit } 2} = g'_2 \ln\left(\frac{b}{b_*}\right). \quad (7)$$

Here  $a_1$  and  $a_2$  in the NP Sudakov factor and  $g_2$  (or  $g'_2$ ) in the NP CS kernel are fit parameters that will be determined by the data. The behavior of Fit 1 was motivated in [72] and applied in [73], albeit with a different choice of  $b_{\max}$ . The parametrization for Fit 2 has been employed in [74, 75]. Both extracted NP CS kernels have been extensively used in phenomenological TMD studies.

**Data Selection.** Within the  $Q$  range of 29.0 GeV to 91.2 GeV, we include EEC data that accounted for both charged and neutral final-state particles, provided statistical and systematic uncertainties or their quadrature sum, and had 50 bins or more across the entire  $\chi$  range. We end up with 8 datasets from collaborations OPAL [16], SLD [14], TOPAZ [17], TASSO [18], MARKII [21], and MAC [20], as summarized in Table I.

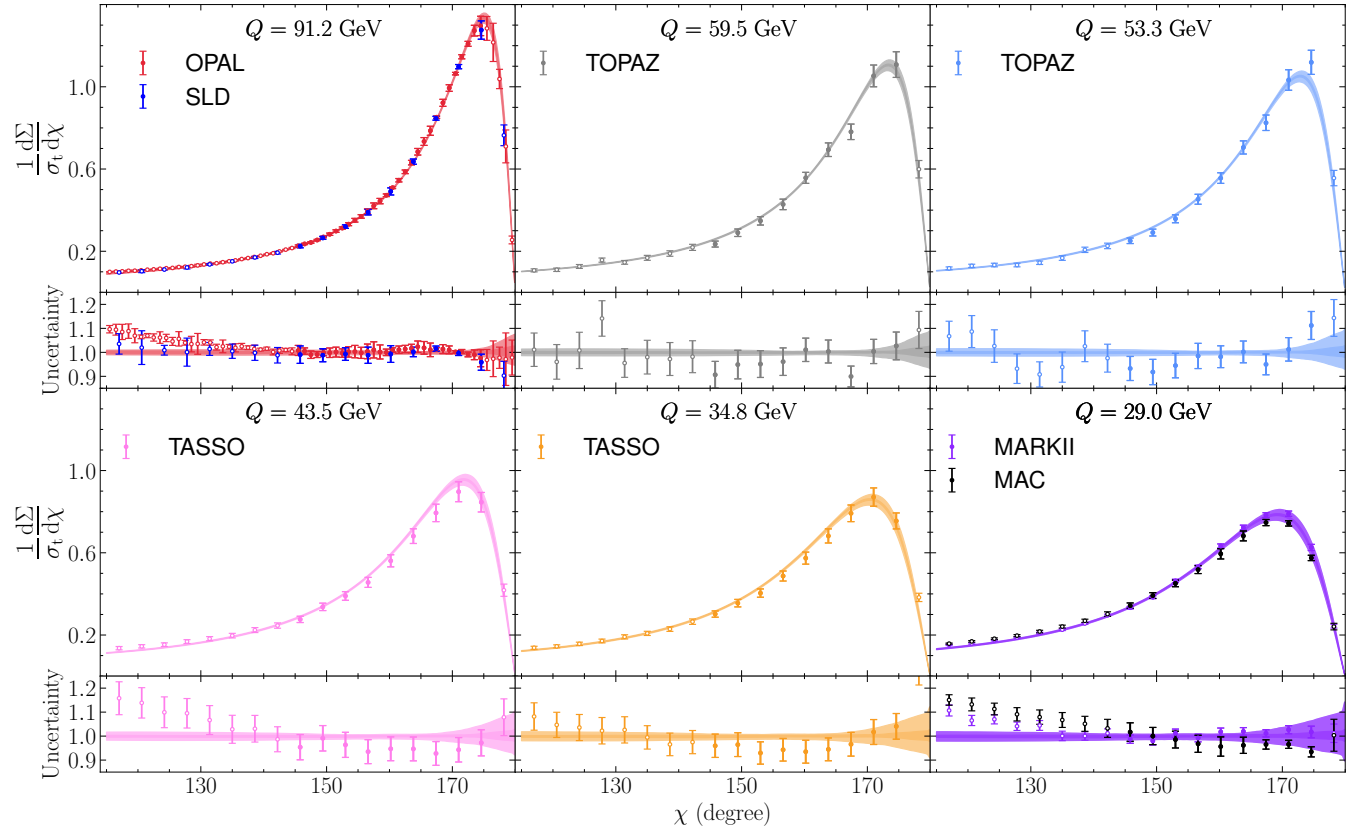


FIG. 1. Comparison of Fit 1’s prediction with central parameters to the experimental data. The dark uncertainty band represents the middle 68% fit uncertainty, and the light band represents the middle 68% theoretical uncertainty. The solid points represent fitted data while empty points are not included in the fit. The total cross-section  $\sigma_t$  is calculated at 2-loop [76].

The fit range is constrained around the peak region of  $145^\circ < \chi < 175^\circ$ .

**Fit Method.** In this Letter, we fit the strong coupling constant  $\alpha_s(m_Z)$ , the NP Sudakov factor, and the NP CS kernel. Therefore, in total we have 4 fitting parameters:  $\alpha_s(m_Z)$ ,  $a_1$ ,  $a_2$ , and  $g_2$ . To obtain optimal parameters, we apply the  $\chi^2$  minimization method. For a given set of parameter values  $\{\mathbf{p}\}$ , the total  $\chi^2(\{\mathbf{p}\}) = \sum_i (T_i(\{\mathbf{p}\}) - E_i)^2 / \sigma_i^2$ . Here, we sum over all experimental data points; for the  $i$ -th data point,  $E_i$  represents the measured EEC, and the uncertainty  $\sigma_i$  equals the quadrature sum of its statistical and systematic uncertainties;  $T_i(\{\mathbf{p}\})$  represents our theoretical prediction for EEC with parameter values  $\{\mathbf{p}\}$ .

**Treatment of Uncertainties.** We account for two sources of uncertainties in our analyses. The first stems from the fit of the strong coupling constant and the parameters of the NP Sudakov factor and the NP CS kernel. We refer to this as the fit uncertainty. To quantify it, we apply the standard replica method [77, 78] using 200 replicas. For each replica, a random Gaussian noise—scaled by the experimental uncertainty—is added to the EEC data points. By fitting the parameters of each replica, we obtain 200 sets of optimal values. The

median value for each parameter serves as the central result, while the upper and lower fit uncertainties correspond to the range that encompasses the central 68% of the parameter values.

Secondly, we account for theoretical uncertainty, which arises from higher-order perturbative corrections in the hard and jet functions. To explore this uncertainty, we use the scan method [79]. In this approach, the initial resummation scales,  $\mu_H^i$ ,  $\zeta_J^i$ , and  $\mu_J^i$ , are varied from their canonical values by random factors within the range  $[\frac{1}{2}, 2]$ . When  $\mu_H^i$  is shifted below its canonical value, we freeze it at 1 GeV for large  $b$  to prevent entering the sub-GeV regime. We generate 200 sets of initial scales and perform fitting using the original experimental data, resulting in 200 sets of optimal parameters. The theoretical uncertainty for each parameter is then determined by the range of the central 68% of these optimal parameter values.

**Numerical Results.** The central parameter values and uncertainties are detailed in Table II, and Fit 1’s prediction is shown in Fig 1. As shown in Table I, both Fit 1 and Fit 2 achieved  $\chi^2/d.o.f = 0.95$ , demonstrating that our model accurately describes the EEC in the back-to-back region ( $145^\circ < \chi < 175^\circ$ ). Additionally, the

	$\alpha_s(m_Z)$	$a_1(\text{GeV}^{a_2})$	$a_2$	$g_2(\text{GeV}^2)$	$g'_2$
Fit 1	$0.1193^{+0.0009+0.0008}_{-0.0009-0.0013}$	$0.530^{+0.060+0.051}_{-0.067-0.052}$	$1.152^{+0.045+0.064}_{-0.049-0.077}$	$0.076^{+0.014+0.015}_{-0.013-0.012}$	N/A
Fit 2	$0.1193^{+0.0010+0.0009}_{-0.0008-0.0013}$	$0.527^{+0.030+0.051}_{-0.036-0.058}$	$1.152^{+0.040+0.065}_{-0.038-0.079}$	N/A	$0.194^{+0.019+0.037}_{-0.020-0.028}$

TABLE II. Central parameter values along with fit and theory uncertainties corresponding to the 68% probability around the median.

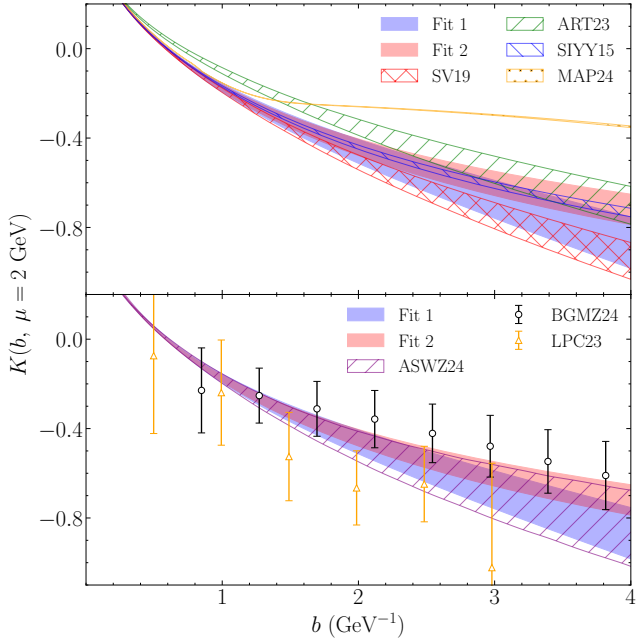


FIG. 2. We compare the full CS kernel  $K(b, \mu = 2 \text{ GeV})$  extracted from EEC (Fit 1 & Fit 2) with other phenomenological extractions in SV19 [73], SIYY15 [74], ART23 [80], and MAP24 [81] on the upper plot, and to lattice QCD results from ASWZ24 [42], BGMZ24 [43], and LPC23 [40] in the lower plot.

model's predictions remain valid in the unfitted region ( $115^\circ < \chi < 145^\circ$ ).

Our extracted value of  $\alpha_s(m_Z)$  aligns closely with the average value  $0.1189 \pm 0.0037$  obtained from  $e^+e^-$  jet and event shape measurements, and is consistent with the Particle Data Group's world average of  $0.1180 \pm 0.0009$  [8] within uncertainty. With  $a_2 = 1.152$ , both fits' NP Sudakov factor are close to linear. We have also checked that fits performed at  $N^3\text{LL}'$  yield central parameter values similar to those at  $N^3\text{LL}$  [32]. For consistent matching with the NLO non-singular contribution, we report only the  $N^3\text{LL}$  results.

Fig. 2 presents the full CS kernel  $K$  extracted from EEC at  $\mu = 2 \text{ GeV}$ , compared against phenomenological extractions [73, 74, 80, 81] (upper panel) and lattice QCD results [35, 42, 81] (lower panel). We display only the fit uncertainty bands to align with other studies. No-

table, ART23 [80] used solely Drell–Yan (DY) process data, while SV19 [73], SIYY15 [74], and MAP24 [42] incorporated both semi-inclusive deep inelastic scattering (SIDIS) and DY. The parametrization of NP CS kernels for SV19 and SIYY15 correspond to those in our Fit 1 and Fit 2, and MAP24's simple quadratic parametrization  $D_{\text{NP}}^{\text{MAP24}} = \tilde{g}_2 b^2$  can also be found in older extractions [77, 82]. ART23's parametrization is  $D_{\text{NP}}^{\text{ART23}} = b b_* (\tilde{g}_2 + \tilde{g}_3 \ln(b_*/b_{\max}))$ . SV19 and ART23 treat  $b_{\max}$  as a fit parameter, while we set  $b_{\max} = 2e^{-\gamma_E} \text{ GeV}^{-1}$ . All three lattice QCD results for the CS kernel were based on quasi TMD wave functions. BGMZ24 [43] and LPC23 [40] reported their CS kernels at discrete  $b$  values, whereas ASWZ24 [42] provided a continuum extrapolation.

Our two extractions of the CS kernel overlap within the 68 % fit uncertainty for  $b < 4 \text{ GeV}^{-1}$ . In comparison with other phenomenological fits, Fit 1 is consistent with SV19, while the uncertainty band of Fit 2 entirely encompasses that of SIYY15. Despite having a different functional form, ART23 also shows reasonable agreement with Fit 2. We note that MAP24 deviates from both our fits and other phenomenological extractions presented in the plot, as well as recent extractions in [83, 84]. When compared to lattice results, the continuum extrapolation from ASWZ24 closely matches our extraction, covering most of the uncertainty bands for both Fit 1 and Fit 2. Additionally, results from BGMZ24 and LPC23 align with our extractions within the 68% uncertainty level.

**Conclusions.** We have analyzed the EEC in  $e^+e^-$  collisions in the back-to-back region using the TMD factorization formalism at  $N^3\text{LL}$  accuracy and, for the first time, performed a simultaneous fit of the strong coupling constant  $\alpha_s(m_Z)$  and the non-perturbative contribution to the Collins–Soper (CS) kernel. Traditionally, the CS kernel has been derived from lattice QCD or phenomenological fits to SIDIS and DY process cross sections. Our method, based on the EEC, offers a cleaner extraction by avoiding the complexities of non-perturbative TMD hadron structures present in conventional SIDIS and DY extractions.

These fits, using two models for the non-perturbative CS kernel, yield strong coupling constants consistent with the world average. Despite slight model-specific dependencies, our CS kernel aligns with lattice QCD results

and most other recent phenomenological extractions. This remarkable alignment offers compelling evidence for the universality of the non-perturbative Collins–Soper kernel, and opens exciting opportunities for joint fits of the EEC experimental data alongside other TMD processes, such as SIDIS and DY production, which are highly promising to be explored at the Large Hadron Collider and the future Electron–Ion Collider.

*Acknowledgments.* This work is supported by the National Science Foundation under grant No. PHY-1945471. This work is also supported by the U.S. Department of Energy, Office of Science, Office of Nuclear Physics, within the framework of the Saturated Glue (SURGE) Topical Theory Collaboration. We thank the lattice groups of [40, 42, 43] for providing lattice data and the group of [81] for providing the phenomenological band.

---

\* zkang@physics.ucla.edu

† janipentala@physics.ucla.edu

‡ maxzhang2002@g.ucla.edu

- [1] D. J. Gross and F. Wilczek, *Ultraviolet Behavior of Nonabelian Gauge Theories*, *Phys. Rev. Lett.* **30** (1973) 1343.
- [2] H. D. Politzer, *Reliable Perturbative Results for Strong Interactions?*, *Phys. Rev. Lett.* **30** (1973) 1346.
- [3] P. A. Baikov, K. G. Chetyrkin and J. H. Kühn, *Five-Loop Running of the QCD coupling constant*, *Phys. Rev. Lett.* **118** (2017) no. 8 082002 [[arXiv:1606.08659 \[hep-ph\]](#)].
- [4] T. Luthe, A. Maier, P. Marquard and Y. Schröder, *Towards the five-loop Beta function for a general gauge group*, *JHEP* **07** (2016) 127 [[arXiv:1606.08662 \[hep-ph\]](#)].
- [5] F. Herzog, B. Ruijl, T. Ueda, J. A. M. Vermaasen and A. Vogt, *The five-loop beta function of Yang-Mills theory with fermions*, *JHEP* **02** (2017) 090 [[arXiv:1701.01404 \[hep-ph\]](#)].
- [6] T. Luthe, A. Maier, P. Marquard and Y. Schröder, *The five-loop Beta function for a general gauge group and anomalous dimensions beyond Feynman gauge*, *JHEP* **10** (2017) 166 [[arXiv:1709.07718 \[hep-ph\]](#)].
- [7] K. G. Chetyrkin, G. Falcioni, F. Herzog and J. A. M. Vermaasen, *Five-loop renormalisation of QCD in covariant gauges*, *JHEP* **10** (2017) 179 [[arXiv:1709.08541 \[hep-ph\]](#)]. [Addendum: *JHEP* **12**, 006 (2017)].
- [8] **Particle Data Group** collaboration, S. Navas *et. al.*, *Review of particle physics*, *Phys. Rev. D* **110** (2024) no. 3 030001.
- [9] R. Abbate, M. Fickinger, A. Hoang, V. Mateu and I. W. Stewart, *Global Fit of  $\alpha_s(M_Z)$  to Thrust at  $N^3LL$  Order with Power Corrections*, *Pos RADCOR2009* (2010) 040 [[arXiv:1004.4894 \[hep-ph\]](#)].
- [10] A. H. Hoang, D. W. Kolodrubetz, V. Mateu and I. W. Stewart, *Precise determination of  $\alpha_s$  from the C-parameter distribution*, *Phys. Rev. D* **91** (2015) no. 9 094018 [[arXiv:1501.04111 \[hep-ph\]](#)].
- [11] **H1** collaboration, V. Andreev *et. al.*, *Determination of the strong coupling constant  $\alpha_s(m_Z)$  in next-to-next-to-leading order QCD using H1 jet cross section measurements*, *Eur. Phys. J. C* **77** (2017) no. 11 791 [[arXiv:1709.07251 \[hep-ex\]](#)]. [Erratum: *Eur. Phys. J. C* **81**, 738 (2021)].
- [12] C. L. Basham, L. S. Brown, S. D. Ellis and S. T. Love, *Energy Correlations in electron - Positron Annihilation: Testing QCD*, *Phys. Rev. Lett.* **41** (1978) 1585.
- [13] C. L. Basham, L. S. Brown, S. D. Ellis and S. T. Love, *Energy Correlations in electron-Positron Annihilation in Quantum Chromodynamics: Asymptotically Free Perturbation Theory*, *Phys. Rev. D* **19** (1979) 2018.
- [14] **SLD** collaboration, K. Abe *et. al.*, *Measurement of alpha-s ( $M(Z)^{**2}$ ) from hadronic event observables at the  $Z_0$  resonance*, *Phys. Rev. D* **51** (1995) 962 [[arXiv:hep-ex/9501003](#)].
- [15] **L3** collaboration, O. Adrián *et. al.*, *Determination of alpha-s from hadronic event shapes measured on the  $Z_0$  resonance*, *Phys. Lett. B* **284** (1992) 471.
- [16] **OPAL** collaboration, P. D. Acton *et. al.*, *An Improved measurement of alpha-s ( $M(Z_0)$ ) using energy correlations with the OPAL detector at LEP*, *Phys. Lett. B* **276** (1992) 547.
- [17] **TOPAZ** collaboration, I. Adachi *et. al.*, *Measurements of  $\alpha^-s$  in  $e^+e^-$  Annihilation at  $\sqrt{s} = 53.3\text{-GeV}$  and  $59.5\text{-GeV}$* , *Phys. Lett. B* **227** (1989) 495.
- [18] **TASSO** collaboration, W. Braunschweig *et. al.*, *A Study of Energy-energy Correlations Between 12-GeV and 46.8-GeV CM Energies*, *Z. Phys. C* **36** (1987) 349.
- [19] **JADE** collaboration, W. Bartel *et. al.*, *Measurements of Energy Correlations in  $e^+e^- \rightarrow$  Hadrons*, *Z. Phys. C* **25** (1984) 231.
- [20] E. Fernandez *et. al.*, *A Measurement of Energy-energy Correlations in  $e^+e^- \rightarrow$  Hadrons at  $\sqrt{s} = 29\text{-GeV}$* , *Phys. Rev. D* **31** (1985) 2724.
- [21] D. R. Wood *et. al.*, *Determination of  $\alpha^-s$  From Energy-energy Correlations in  $e^+e^-$  Annihilation at 29-GeV*, *Phys. Rev. D* **37** (1988) 3091.
- [22] **CELLO** collaboration, H. J. Behrend *et. al.*, *Analysis of the Energy Weighted Angular Correlations in Hadronic  $e^+e^-$  Annihilations at 22-GeV and 34-GeV*, *Z. Phys. C* **14** (1982) 95.
- [23] **PLUTO** collaboration, C. Berger *et. al.*, *A Study of Energy-energy Correlations in  $e^+e^-$  Annihilations at  $\sqrt{s} = 34.6\text{-GeV}$* , *Z. Phys. C* **28** (1985) 365.
- [24] **OPAL** collaboration, M. Z. Akrawy *et. al.*, *A Measurement of energy correlations and a determination of alpha-s ( $M_2(Z_0)$ ) in  $e + e -$  annihilations at  $s^{**}(1/2) = 91\text{-GeV}$* , *Phys. Lett. B* **252** (1990) 159.
- [25] **ALEPH** collaboration, D. Decamp *et. al.*, *Measurement of alpha-s from the structure of particle clusters produced in hadronic Z decays*, *Phys. Lett. B* **257** (1991) 479.
- [26] **L3** collaboration, B. Adeva *et. al.*, *Determination of alpha-s from energy-energy correlations measured on the  $Z_0$  resonance*, *Phys. Lett. B* **257** (1991) 469.
- [27] **SLD** collaboration, K. Abe *et. al.*, *Measurement of alpha-s from energy-energy correlations at the  $Z_0$  resonance*, *Phys. Rev. D* **50** (1994) 5580 [[arXiv:hep-ex/9405006](#)].
- [28] **CMS** collaboration, A. Hayrapetyan *et. al.*, *Measurement of Energy Correlators inside Jets and Determination of the Strong Coupling  $\alpha S(mZ)$* , *Phys. Rev. Lett.* **133** (2024) no. 7 071903 [[arXiv:2402.13864](#)]

- [hep-ex]].
- [29] ALICE collaboration, S. Acharya *et. al.*, *Exposing the parton-hadron transition within jets with energy-energy correlators in pp collisions at  $\sqrt{s} = 5.02$  TeV*, [arXiv:2409.12687 \[hep-ex\]](#).
- [30] D. Neill, G. Vita, I. Vitev and H. X. Zhu in *Snowmass 2021*, 3, 2022. [arXiv:2203.07113 \[hep-ph\]](#).
- [31] X. Liu, W. Vogelsang, F. Yuan and H. X. Zhu, *Universality in the Near-Side Energy-Energy Correlator*, [arXiv:2410.16371 \[hep-ph\]](#).
- [32] M. A. Ebert, B. Mistlberger and G. Vita, *The Energy-Energy Correlation in the back-to-back limit at  $N^3LO$  and  $N^3LL'$* , *JHEP* **08** (2021) 022 [[arXiv:2012.07859 \[hep-ph\]](#)].
- [33] L. J. Dixon, I. Moult and H. X. Zhu, *Collinear limit of the energy-energy correlator*, *Phys. Rev. D* **100** (2019) no. 1 014009 [[arXiv:1905.01310 \[hep-ph\]](#)].
- [34] J. Collins, *Foundations of Perturbative QCD*, vol. 32 of *Cambridge Monographs on Particle Physics, Nuclear Physics and Cosmology*. Cambridge University Press, 7, 2023.
- [35] R. Boussarie *et. al.*, *TMD Handbook*, [arXiv:2304.03302 \[hep-ph\]](#).
- [36] H.-T. Shu, M. Schlemmer, T. Sizmann, A. Vladimirov, L. Walter, M. Engelhardt, A. Schäfer and Y.-B. Yang, *Universality of the Collins-Soper kernel in lattice calculations*, *Phys. Rev. D* **108** (2023) no. 7 074519 [[arXiv:2302.06502 \[hep-lat\]](#)].
- [37] P. Shanahan, M. Wagman and Y. Zhao, *Collins-Soper kernel for TMD evolution from lattice QCD*, *Phys. Rev. D* **102** (2020) no. 1 014511 [[arXiv:2003.06063 \[hep-lat\]](#)].
- [38] Lattice Parton collaboration, Q.-A. Zhang *et. al.*, *Lattice-QCD Calculations of TMD Soft Function Through Large-Momentum Effective Theory*, *Phys. Rev. Lett.* **125** (2020) no. 19 192001 [[arXiv:2005.14572 \[hep-lat\]](#)].
- [39] Lattice Parton (LPC) collaboration, M.-H. Chu *et. al.*, *Nonperturbative determination of the Collins-Soper kernel from quasitransverse-momentum-dependent wave functions*, *Phys. Rev. D* **106** (2022) no. 3 034509 [[arXiv:2204.00200 \[hep-lat\]](#)].
- [40] Lattice Parton (LPC) collaboration, M.-H. Chu *et. al.*, *Lattice calculation of the intrinsic soft function and the Collins-Soper kernel*, *JHEP* **08** (2023) 172 [[arXiv:2306.06488 \[hep-lat\]](#)].
- [41] A. Avkhadiev, P. E. Shanahan, M. L. Wagman and Y. Zhao, *Collins-Soper kernel from lattice QCD at the physical pion mass*, *Phys. Rev. D* **108** (2023) no. 11 114505 [[arXiv:2307.12359 \[hep-lat\]](#)].
- [42] A. Avkhadiev, P. E. Shanahan, M. L. Wagman and Y. Zhao, *Determination of the Collins-Soper Kernel from Lattice QCD*, *Phys. Rev. Lett.* **132** (2024) no. 23 231901 [[arXiv:2402.06725 \[hep-lat\]](#)].
- [43] D. Bollweg, X. Gao, S. Mukherjee and Y. Zhao, *Nonperturbative Collins-Soper kernel from chiral quarks with physical masses*, *Phys. Lett. B* **852** (2024) 138617 [[arXiv:2403.00664 \[hep-lat\]](#)].
- [44] A. Accardi *et. al.*, *Electron Ion Collider: The Next QCD Frontier: Understanding the glue that binds us all*, *Eur. Phys. J. A* **52** (2016) no. 9 268 [[arXiv:1212.1701 \[nucl-ex\]](#)].
- [45] E. C. Aschenauer, S. Fazio, J. H. Lee, H. Mantysaari, B. S. Page, B. Schenke, T. Ullrich, R. Venugopalan and P. Zurita, *The electron-ion collider: assessing the energy dependence of key measurements*, *Rept. Prog. Phys.* **82** (2019) no. 2 024301 [[arXiv:1708.01527 \[nucl-ex\]](#)].
- [46] R. Abdul Khalek *et. al.*, *Science Requirements and Detector Concepts for the Electron-Ion Collider: EIC Yellow Report*, *Nucl. Phys. A* **1026** (2022) 122447 [[arXiv:2103.05419 \[physics.ins-det\]](#)].
- [47] L. J. Dixon, M.-X. Luo, V. Shtabovenko, T.-Z. Yang and H. X. Zhu, *Analytical Computation of Energy-Energy Correlation at Next-to-Leading Order in QCD*, *Phys. Rev. Lett.* **120** (2018) no. 10 102001 [[arXiv:1801.03219 \[hep-ph\]](#)].
- [48] Z. Tulipánt, A. Kardos and G. Somogyi, *Energy-energy correlation in electron-positron annihilation at NNLL + NNLO accuracy*, *Eur. Phys. J. C* **77** (2017) no. 11 749 [[arXiv:1708.04093 \[hep-ph\]](#)].
- [49] T. Becher and M. D. Schwartz, *A precise determination of  $\alpha_s$  from LEP thrust data using effective field theory*, *JHEP* **07** (2008) 034 [[arXiv:0803.0342 \[hep-ph\]](#)].
- [50] Y. Li and H. X. Zhu, *Bootstrapping Rapidity Anomalous Dimensions for Transverse-Momentum Resummation*, *Phys. Rev. Lett.* **118** (2017) no. 2 022004 [[arXiv:1604.01404 \[hep-ph\]](#)].
- [51] M. A. Ebert, B. Mistlberger and G. Vita, *Transverse momentum dependent PDFs at  $N^3LO$* , *JHEP* **09** (2020) 146 [[arXiv:2006.05329 \[hep-ph\]](#)].
- [52] M.-x. Luo, T.-Z. Yang, H. X. Zhu and Y. J. Zhu, *Quark Transverse Parton Distribution at the Next-to-Next-to-Next-to-Leading Order*, *Phys. Rev. Lett.* **124** (2020) no. 9 092001 [[arXiv:1912.05778 \[hep-ph\]](#)].
- [53] T. Lübbert, J. Oredsson and M. Stahlhofen, *Rapidity renormalized TMD soft and beam functions at two loops*, *JHEP* **03** (2016) 168 [[arXiv:1602.01829 \[hep-ph\]](#)].
- [54] A. A. Vladimirov, *Correspondence between Soft and Rapidity Anomalous Dimensions*, *Phys. Rev. Lett.* **118** (2017) no. 6 062001 [[arXiv:1610.05791 \[hep-ph\]](#)].
- [55] O. V. Tarasov, A. A. Vladimirov and A. Y. Zharkov, *The Gell-Mann-Low Function of QCD in the Three Loop Approximation*, *Phys. Lett. B* **93** (1980) 429.
- [56] S. A. Larin and J. A. M. Vermaasen, *The Three loop QCD Beta function and anomalous dimensions*, *Phys. Lett. B* **303** (1993) 334 [[arXiv:hep-ph/9302208](#)].
- [57] T. van Ritbergen, J. A. M. Vermaasen and S. A. Larin, *The Four loop beta function in quantum chromodynamics*, *Phys. Lett. B* **400** (1997) 379 [[arXiv:hep-ph/9701390](#)].
- [58] M. Czakon, *The Four-loop QCD beta-function and anomalous dimensions*, *Nucl. Phys. B* **710** (2005) 485 [[arXiv:hep-ph/0411261](#)].
- [59] G. P. Korchemsky and A. V. Radyushkin, *Renormalization of the Wilson Loops Beyond the Leading Order*, *Nucl. Phys. B* **283** (1987) 342.
- [60] J. M. Henn, G. P. Korchemsky and B. Mistlberger, *The full four-loop cusp anomalous dimension in  $\mathcal{N} = 4$  super Yang-Mills and QCD*, *JHEP* **04** (2020) 018 [[arXiv:1911.10174 \[hep-th\]](#)].
- [61] S. Moch, J. A. M. Vermaasen and A. Vogt, *The Three loop splitting functions in QCD: The Nonsinglet case*, *Nucl. Phys. B* **688** (2004) 101 [[arXiv:hep-ph/0403192](#)].
- [62] A. Vogt, S. Moch and J. A. M. Vermaasen, *The Three-loop splitting functions in QCD: The Singlet case*, *Nucl. Phys. B* **691** (2004) 129 [[arXiv:hep-ph/0404111](#)].

- [63] J. Henn, A. V. Smirnov, V. A. Smirnov, M. Steinhauser and R. N. Lee, *Four-loop photon quark form factor and cusp anomalous dimension in the large- $N_c$  limit of QCD*, *JHEP* **03** (2017) 139 [[arXiv:1612.04389 \[hep-ph\]](#)].
- [64] S. Moch, B. Ruijl, T. Ueda, J. A. M. Vermaasen and A. Vogt, *Four-Loop Non-Singlet Splitting Functions in the Planar Limit and Beyond*, *JHEP* **10** (2017) 041 [[arXiv:1707.08315 \[hep-ph\]](#)].
- [65] R. N. Lee, A. V. Smirnov, V. A. Smirnov and M. Steinhauser, *Four-loop quark form factor with quartic fundamental colour factor*, *JHEP* **02** (2019) 172 [[arXiv:1901.02898 \[hep-ph\]](#)].
- [66] J. M. Henn, T. Peraro, M. Stahlhofen and P. Wasser, *Matter dependence of the four-loop cusp anomalous dimension*, *Phys. Rev. Lett.* **122** (2019) no. 20 201602 [[arXiv:1901.03693 \[hep-ph\]](#)].
- [67] R. Brüser, A. Grozin, J. M. Henn and M. Stahlhofen, *Matter dependence of the four-loop QCD cusp anomalous dimension: from small angles to all angles*, *JHEP* **05** (2019) 186 [[arXiv:1902.05076 \[hep-ph\]](#)].
- [68] A. von Manteuffel, E. Panzer and R. M. Schabinger, *Cusp and collinear anomalous dimensions in four-loop QCD from form factors*, *Phys. Rev. Lett.* **124** (2020) no. 16 162001 [[arXiv:2002.04617 \[hep-ph\]](#)].
- [69] J. C. Collins, D. E. Soper and G. F. Sterman, *Transverse Momentum Distribution in Drell-Yan Pair and W and Z Boson Production*, *Nucl. Phys. B* **250** (1985) 199.
- [70] J. Collins and T. Rogers, *Understanding the large-distance behavior of transverse-momentum-dependent parton densities and the Collins-Soper evolution kernel*, *Phys. Rev. D* **91** (2015) no. 7 074020 [[arXiv:1412.3820 \[hep-ph\]](#)].
- [71] Z.-B. Kang, S. Lee, J. Penttala, F. Zhao and Y. Zhou, *Transverse Energy-Energy Correlator for Vector Boson-Tagged Hadron Production in pp and pA collisions*, [arXiv:2410.02747 \[hep-ph\]](#).
- [72] A. A. Vladimirov, *Self-contained definition of the Collins-Soper kernel*, *Phys. Rev. Lett.* **125** (2020) no. 19 192002 [[arXiv:2003.02288 \[hep-ph\]](#)].
- [73] I. Scimemi and A. Vladimirov, *Non-perturbative structure of semi-inclusive deep-inelastic and Drell-Yan scattering at small transverse momentum*, *JHEP* **06** (2020) 137 [[arXiv:1912.06532 \[hep-ph\]](#)].
- [74] P. Sun, J. Isaacson, C. P. Yuan and F. Yuan, *Nonperturbative functions for SIDIS and Drell-Yan processes*, *Int. J. Mod. Phys. A* **33** (2018) no. 11 1841006 [[arXiv:1406.3073 \[hep-ph\]](#)].
- [75] M. G. Echevarria, Z.-B. Kang and J. Terry, *Global analysis of the Sivers functions at NLO+NNLL in QCD*, *JHEP* **01** (2021) 126 [[arXiv:2009.10710 \[hep-ph\]](#)].
- [76] A. Kardos, S. Kluth, G. Somogyi, Z. Tulipán and A. Verbytskyi, *Precise determination of  $\alpha_S(M_Z)$  from a global fit of energy-energy correlation to NNLO+NNLL predictions*, *Eur. Phys. J. C* **78** (2018) no. 6 498 [[arXiv:1804.09146 \[hep-ph\]](#)].
- [77] A. Bacchetta, F. Delcarro, C. Pisano, M. Radici and A. Signori, *Extraction of partonic transverse momentum distributions from semi-inclusive deep-inelastic scattering, Drell-Yan and Z-boson production*, *JHEP* **06** (2017) 081 [[arXiv:1703.10157 \[hep-ph\]](#)]. [Erratum: JHEP 06, 051 (2019)].
- [78] M. Alrashed, Z.-B. Kang, J. Terry, H. Xing and C. Zhang, *Nuclear modified transverse momentum dependent parton distribution and fragmentation functions*, [arXiv:2312.09226 \[hep-ph\]](#).
- [79] G. Bell, C. Lee, Y. Makris, J. Talbert and B. Yan, *Effects of renormalon scheme and perturbative scale choices on determinations of the strong coupling from e+e- event shapes*, *Phys. Rev. D* **109** (2024) no. 9 094008 [[arXiv:2311.03990 \[hep-ph\]](#)].
- [80] V. Moos, I. Scimemi, A. Vladimirov and P. Zurita, *Extraction of unpolarized transverse momentum distributions from the fit of Drell-Yan data at  $N^4 LL$* , *JHEP* **05** (2024) 036 [[arXiv:2305.07473 \[hep-ph\]](#)].
- [81] MAP collaboration, A. Bacchetta, V. Bertone, C. Bissolotti, G. Bozzi, M. Cerutti, F. Delcarro, M. Radici, L. Rossi and A. Signori, *Flavor dependence of unpolarized quark transverse momentum distributions from a global fit*, *JHEP* **08** (2024) 232 [[arXiv:2405.13833 \[hep-ph\]](#)].
- [82] MAP (Multi-dimensional Analyses of Partonic distributions) collaboration, A. Bacchetta, V. Bertone, C. Bissolotti, G. Bozzi, M. Cerutti, F. Piacenza, M. Radici and A. Signori, *Unpolarized transverse momentum distributions from a global fit of Drell-Yan and semi-inclusive deep-inelastic scattering data*, *JHEP* **10** (2022) 127 [[arXiv:2206.07598 \[hep-ph\]](#)].
- [83] J. Isaacson, Y. Fu and C. P. Yuan, *Improving resbos for the precision needs of the LHC*, *Phys. Rev. D* **110** (2024) no. 7 073002 [[arXiv:2311.09916 \[hep-ph\]](#)].
- [84] F. Aslan, M. Boglione, J. O. Gonzalez-Hernandez, T. Rainaldi, T. C. Rogers and A. Simonelli, *Phenomenology of TMD parton distributions in Drell-Yan and Z0 boson production in a hadron structure oriented approach*, *Phys. Rev. D* **110** (2024) no. 7 074016 [[arXiv:2401.14266 \[hep-ph\]](#)].